 doi:10.20944/preprints202012.0542.v1

Article

Evaluation of image-based phenotyping methods for measuring water yam (*Dioscorea alata* L.) growth and nitrogen nutritional status under greenhouse and field conditions

Emmanuel Frossard [*#1], Frank Liebisch [#2,3], Valerie K Hgaza [4,5], Delwende I Kiba [1,6], Norbert Kirchgessner [2], Laurin Müller [1,2], Patrick Müller [1,2], Nestor Pouya [7], Cecil Ringger [1,2,3], Achim Walter [2]

[1] Group of Plant Nutrition, Institute of Agricultural Sciences, ETH Zurich, Switzerland; emmanuel.frossard@usys.ethz.ch; delwende.kiba@usys.ethz.ch; muellaur@gmail.com; mupatric@student.ethz.ch
[2] Group of Crop Science, Institute of Agricultural Sciences, ETH Zurich, Switzerland; frank.liebisch@usys.ethz.ch; norbert.kirchgessner@usys.ethz.ch; achim.walter@usys.ethz.ch
[3] Agroscope, Zürich, Switzerland; frank.liebisch@agroscope.admin.ch; cecil.ringger@agroscope.admin.ch
[4] Centre Suisse de Recherches Scientifiques, Abidjan, Côte d'Ivoire; hgaza.kouame@csrs.ci
[5] Département d'Agrophysiologie des Plantes, Université Peleforo Gon Coulibaly, Korhogo, Côte d'Ivoire;
6 Institut de l'Environnement et Recherches Agricoles, Ouagadougou, Burkina Faso;
[7] Laboratory of Plant Physiology, Université Félix Houphouët Boigny, Abidjan, Côte d'Ivoire; nestaledja@gmail.com
[*] Correspondence: emmanuel.frossard@usys.ethz.ch; Tel +41 52 354 91 40
[#] Both first authors (EF, FL) have contributed in the same manner to this paper

Abstract: Management practices must be developed to improve yam production sustainability. Image-based phenotyping techniques could help developing such practices based on non-destructive analyses of important plant traits. Our objective was to determine the potential of image-based phenotyping methods to assess traits relevant for tuber yield formation in yam grown in glasshouse and field. We took plant and leaf pictures with consumer cameras. We used the numbers of image pixels to derive the shoot biomass and the total leaf surface and calculated the 'triangular greenness index' (TGI) which is an indicator of the plant nitrogen (N) nutritional status. Under glasshouse conditions, the number of pixels obtained from nadir view (image taken top down) was positively correlated to the shoot biomass, and the total leaf surface, while the TGI was negatively correlated to the N content of diagnostic leaves. Under field conditions, pictures taken from the nadir view showed an increase in soil surface cover and a decrease in TGI with time. TGI was negatively correlated to SPAD measured on specific leaves but was not correlated to the N content of these leaves. In conclusion, these phenotyping techniques deliver relevant results but need to be further developed and validated for application in yam.

Keywords: Leaf surface; soil surface cover; growth rate; nitrogen leaf content; SPAD; triangular greenness index (TGI)

1. Introduction

The yam genus (*Dioscorea* spp) has 640 species, twelve of them being cultivated and used as staple food by millions of people in tropical areas [1]. Besides being a staple food, yams are a source of income for the actors of the yam value-chain, yams are used in traditional medicine, they are a source of metabolites for the pharmaceutical industry, and they are often part of the local people's cultures [1-3].

West Africa produces more than 90% of the world tuber production over 8.5 million of hectares [1]. The increase in yam tuber production observed in West Africa during the last 60 years was made possible by an increase in cultivated surfaces and not by an increase in tuber yields [4]. The average tuber production in West Africa remains low (around 10 t fresh tuber ha^{-1}) compared to 50 t fresh tuber ha^{-1} that can be produced under well-managed conditions [5]. The traditional yam cropping practices of West Africa largely explain this low productivity. Yams are traditionally planted by small holders in slash and burn systems following either long or short-term fallows without any external inputs, with low quality planting material and at low planting density. Low soil fertility, bad planting material, high pest, and disease pressure, and decreasing and erratic rainfall distribution are major yield limiting factors [1,4,6]. As population is still growing at a fast pace in West Africa, yam tuber demand will probably further increase. Therefore, it is urgent to develop cropping practices to sustainably increase the productivity of this under-researched crop [6].

Important traits for tuber yield formation are i) the emergence rate as the first emerged plants contribute most to the final tuber yield measured at field level [7,8], ii) the foliage development as maximum leaf area index is correlated to final tuber yield [9] due to improved light interception, and limited weed infestation and soil erosion [5], and iii) the N nutritional status, because N leaf status is one of the main factors driving leaf formation and growth [9]. Conducting field experiments to study these factors requires large fields, a lot of time and labor. Indeed, in such experiments yams are planted at a density of one plant per m^2, the leaf area index can reach values of up to eight, this plant can reach a height of several meters if it finds a climbing support and the growth period may last nine months. Classically, destructive sampling is used to measure plant biomass, leaf surface and N uptake [9]. However, given the variability that exists between individual plants [7], destructive sampling further increases the variability of results, which decreases our ability to statistically detect differences associated with specific treatments. Following single plants during the growing season with non-destructive methods could therefore be useful to study more precisely the impacts of specific treatments on yam growth under field conditions.

Image-based phenotyping is widely used to analyze plant traits such as germination rate, leaf surface, and growth rate of cereals and legumes [10-13]. More recently image-based phenotyping was successfully adapted for root and tuber crops such as sugar beet and potato [14-17]. Serial imaging, by Red Green Blue (RGB) cameras (consumer cameras) coupled with appropriate segmentation techniques and image analysis delivers information on plant growth, and soil cover. In addition, the leaf spectral indices derived from the visible and near-infrared ranges of the light spectrum, such as the triangular greenness index (TGI), provide information on the chlorophyll content and N nutrition status of crops [12,18]. Such imaging approaches could be useful for studying yam growth under field conditions.

There is little information on the use of image-based phenotyping to assess the growth, biomass and N nutritional status of tropical root and tuber crops. Phenotyping of these crops is challenging as they have often a more complex morphology and growth habitus than temperate crops such as wheat, maize and soybean. Iseki and Matsumoto [19] developed a model for shoot dry matter production of a white guinea yam (*D. rotundata*) cultivar grown over several months using a sensor measuring the green area of the plant and the plant height. The model underestimated dry plant weight when it was higher than 150 g and the predicted biomass showed a high variability. This model did not predict leaf surface nor the N plant content. Other authors have used image analysis to assess the prevalence of diseases on leaves of yam and cassava [20-22].

The objective of this paper is to determine the potential of image-based phenotyping methods to assess yam traits that are relevant for tuber yield formation. The traits considered in this paper were leaf surface, shoot biomass, and the plant N status measured until six to nine weeks after emergence. This work focused on water yam (*D. alata*) because it is grown all over the tropics. Since published information on yam phenotyping methodology is scarce, we first analyzed the feasibility of detecting the above-mentioned traits under greenhouse conditions by comparing data derived

Preprints (www.preprints.org) | NOT PEER-REVIEWED | Posted: 21 December 2020 doi:10.20944/preprints202012.0542.v1

from the phenotyping approaches to those measured with classical methods and subsequently we tested the imaging approach in a field experiment conducted in Tieningboué, in the center of Côte d'Ivoire.

2. Materials and Methods

2.1. Greenhouse experiments

We conducted two greenhouse experiments at the ETH Zurich plant research station in Eschikon (47°26'N 8°40'E, 520 m above sea level). The first was conducted from July to October 2015 by Ringger [23], and the second from December 2016 to March 2017 by Müller [24]. Since both experiments delivered similar results, although they were based on slightly different designs, we only present and discuss the 2nd experiment in the main part of this paper. The materials and methods and the main results of the 1st experiment are shown in the 1st part of the supplementary materials.

2.1.1. Plant material, growth conditions and experimental design

We grew the water yam cultivar "raja ala" from Sri Lanka, which was imported to Zurich by SK Trading GmbH, Zurich, Switzerland. We used the minisett technique to install the experiment [25]. Head parts of healthy-looking tubers were cut into minisetts of about 70 g fresh weight. Each minisett was dipped for ten minutes in a fungicide solution of 2.5 g MALVIN® WG per liter water (active substance captan) before being planted. One minisett was planted per pot at 8 to 10 cm depth, with the peel (periderm) facing downwards.

A total of 60 minisetts were planted into black plastic pots (2.9 l volume, 16 cm diameter, 18 cm height), filled with 1.0 kg substrate (dry weight). The substrate, a coarse grained attapulgite clay granulate (Oil-Dri US-Special, Oilbinder Type III R, Damolin Mettmann GmbH, Oberhausen, Germany) was selected for its low total N content (0.3 g kg^{-1} substrate), good structure, and high water holding capacity. Four wooden sticks were installed on the edge of each pot and growing vines were trained around them. To facilitate image analysis the sticks were painted in blue. Plants were irrigated with tap water every second to third day. Temperature ranged between 24°C and 27°C during the day and between 20°C and 22°C during the night. Relative atmospheric humidity was 60% during the day and 65% during the night. Metal-halid lamps (Type PF400S, Hugentobler Spezialleuchten AG, Weinfelden Switzerland) were adjusted 1.80 m above the greenhouse table, to ensure a photoperiod of 12 h d^{-1} at 30 kLux.

As yam tuber sprouting is variable [7], we decided to arrange the pot experiment in three blocks based on the emergence date of the plants. The 20 plants that emerged first formed block one, the following plants that emerged 21st – 40th built block two and the last 20 plants built block three. All plants of block one and two emerged within five days each. In block three, 19 out of 20 plants emerged within eight days while the last one emerged ten days after the first emerged plant of block three. The median of all plants per block was selected as emergence date per block. All plants were arranged randomly within each block.

Each block included four N levels: 0, 101, 202 and 342 mg N pot^{-1} (equivalent to 0, 50, 100 and 170 kg N ha^{-1}) which were replicated five times each. These N fertilization rates were supposed to trigger large differences in plant growth and N content. Nitrogen was applied in form of calcium nitrate ($Ca(NO_3)_2$). The application of the 50 and 100 kg N ha^{-1} treatment was made two weeks after the corresponding emergence date per block. The 170 kg N ha^{-1} treatment was split into two doses of each 85 kg N ha^{-1} applied 14 and 28 days after emergence. Additionally, each plant received sufficient phosphorus (KH_2PO_4), potassium (K_2SO_4), zinc ($ZnSO_4$) and iron (Fe-Sequestrene) added in a nutrient solution two weeks after emergence. None of the nutrient deficiency symptoms described by O'Sullivan and Jenner [26] were observed during the experiment. Plants did not show any visible signs of diseases or pest attacks during their growth.

2.1.2. Sampling and measurements

Preprints (www.preprints.org) | NOT PEER-REVIEWED | Posted: 21 December 2020 doi:10.20944/preprints202012.0542.v1

We describe here the destructive and non-destructive samplings. The imaging techniques are presented in section 2.3.

2.1.2.1. Destructive sampling for biomass production and leaf N content

Destructive sampling took place three, six and nine weeks after emergence. Block one was harvested after 61 days, block two was harvested after 40 days, while block three was harvested after 20 days. For destructive sampling, all plants of the corresponding block were cut at the level of soil surface. After petioles and leaves were detached from the vines, total vine length was measured. Total fresh shoot biomass (vine, petiole, and leaves) was weighed and dried at 55°C for at least one week to obtain the total shoot dry weight.

The N concentrations of selected leaves were determined by separating the 1st and 7th fully developed leaves counted from the apex of each vine at each harvest. These leaves were first analyzed by imaging (see section 2.3). Afterwards the leaves were dried at 50°C for two days and powdered with a ball mill (Mixer Mill MM200, Retsch GmbH, Haan, Germany). Nitrogen concentration in leaves was determined by flash combustion using a Flash EA 1112 NC analyzer (Thermo Fisher Scientific, Waltham, MA, USA).

2.1.2.2. Non-destructive sampling for leaf number and SPAD values analysis

The total number of leaves was counted weekly, a day before images were taken. Every week the most recently counted leaf was marked with a string and counting continued the week after starting with the marked leaf. Since leaves of water yam can have an alternate and an opposite arrangement on the vine [26] we counted each node as one leaf regardless if leaves had developed in opposite or alternate order. SPAD values [27,28] were only measured on the 7th leaf starting from the apex using a SPAD meter (SPAD-502, Minolta Corporation, 130 Ramsey, NJ, USA) as the leaf in the first position was generally too small for these measures. Typically, three SPAD measures were taken per leaf and then averaged.

2.2. Field experiment

The field experiment was conducted by Müller [29]. We present thereafter the site, the experimental design, the installation of the field experiment and the methods used. The imaging techniques are presented in section 2.3.

2.2.1. Site description

In May 2018, a field experiment was installed in Tieningboué, Côte d'Ivoire (8°11′N 5°43′W, 317 m above sea level) on an acric plinthic Ferralsol [30,31]. The upper horizon of this soil (0-22 cm) contained 140 g clay kg^{-1} soil, 6.7 g C kg^{-1} soil, 0.47 g N kg^{-1} soil and had a pH in water of 5.1 [31]. The site is located in the Center of Côte d'Ivoire, in the Béré region, department of Mankono. The area of Tieningboué is characterized by a tropical climate with a dry season (October to February) and a rainy season (March to September). The climatic data of the season 2018 were recorded with a Campbell Scientific CR1000 weather station and are shown in the supplementary material (Figure S2.1).

2.2.2. Experimental design

We tested the use of image-based phenotyping in a single block of a large field experiment assessing the impact of crop rotation and fertilization on yam growth. The trial was started in 2016 and was in its 3rd year. The four studied rotations were water yam – rice – water yam (R1), water yam – groundnut – water yam (R2), water yam intercropped with maize – rice – water yam (R3), and water yam – white guinea yam – water yam (R4). There were four fertilization treatments T0, T1, T2 and T3. The treatment T0 (no fertilization) received no nutrient input. The treatment T1 (fully mineral) received NPK for a target yield of 25 t fresh tuber ha^{-1} (56 kg N ha^{-1}, 8 kg P ha^{-1}, 80 kg K ha^{-1}) in the form of mineral fertilizers (urea, super triple phosphate, K_2SO_4). The treatment T2 (organo-mineral)

 doi:10.20944/preprints202012.0542.v1

received half of the NPK added as mineral fertilizers plus poultry manure added at the rate of 3.9 t manure fresh weight ha^{-1} bringing 76, 41 and 50 kg N, P, and K (total elements) ha^{-1}. The treatment T3 (fully organic) received only poultry manure at the rate of 7.8 t ha^{-1}, bringing 152, 82 and 100 kg N, P, and K ha^{-1}. The mineral fertilizers (NPK) were broadcasted at equal doses on July 10 and on August 29 2018 for T1. In T2, manure was added on May 22 2018 just before mound preparation, while mineral NPK fertilizers were broadcasted on August 29. Finally, in T3 the manure was also added on May 22 2018 before preparing the mound.

The image-based phenotyping was tested on each one of the following combinations (R1T0, R1T1, R1T2, R1T3, R2T0, R2T1, R2T2, R2T3, R3T0, R3T1, R3T2, R3T3, R4T0, R4T1, R4T2, R4T3) on two plants per plot making a total of 16 plots or 32 plants. We had no replicated treatment in this imaging experiment. With this design we wanted to trigger a large variation in early growth traits such as soil surface cover by yam shoots, and leaf N content.

2.2.3. Installation of the field experiment

We used the water yam cultivar C18 bred by IITA, that is currently spreading in West Africa [32]. Healthy tubers were selected and cut in setts of 200 g fresh weight. These setts were dipped in a suspension containing wood ash (15 g L^{-1}) and the fungicide mancozeb (12 g L^{-1}) for 10 minutes and dried for 24 hours in the shade. Wood ash is considered by local farmers to be an effective insecticide/nematicide [6]. Fifty cm high mounds were prepared at a density of one mound per square meter. The setts were inserted within the center of mound at 20 cm depth. A single plot (4 m by 5 m) was composed of six central plants installed in two rows of three plants surrounded by 14 border plants. Two of the central plants were used for imaging (see section 2.3). Head parts of tuber setts were used as planting material for the six central plants to ensure a homogeneous germination, while other parts of tuber setts were used for the border plants. Each plot was separated from the next one by a distance of 1.5 m. Planting was done on May 29 2018, 80% of the central plants had germinated on June 28 2018, tuber initiation was reached around August 20 2018, and tubers were harvested on December 12 2018. Manual weeding was organized both to limit competition between yams and other plants and to avoid problems for later image analysis caused by non-yam vegetation. Plants did not show visible symptoms of diseases or signs of pest attacks during their growth.

2.2.4. Sampling and measurements

Tuber yields could not be measured on our 16 plots, but they were measured on the four neighboring blocks located 20 m away from our plots (so on the same soil and submitted to the same climate), studying the effects of the same rotations and fertilizations treatments on the C18 cultivar.

Soil surface cover by leaves and plant TGI were measured from July 5 to August 10, 2018 by imaging (see section 2.3). Leaves located between the 6th and 8th positions from the apex of the main vine were marked and used to measure the SPAD values as described above [27]. Five readings were taken and the mean SPAD-value per leaf was calculated using the device's integrated average function. Leaves were sampled after SPAD measurement, dried in an oven at 50°C for two days and powdered with a ball mill (Mixer Mill MM200, Retsch GmbH, Haan, Germany). Nitrogen concentration in leaves was finally determined by flash combustion using a Flash EA 1112 NC analyzer (Thermo Fisher Scientific, Waltham, MA, USA). SPAD values were measured on July 14, August 8 and 10 2018, while N leaf content was measured only on August 8 and 10. SPAD and leaf N contents were measured on the plants that were analyzed by imaging.

2.3. Imaging devices, acquisition, and analysis

2.3.1. Imaging in the greenhouse experiment

Images were taken in the greenhouse studies with a custom-made indoor imaging station consisting of a blue background and two cameras for top down (nadir view) and side view, respectively (Figure 1). Two blue plastic plates (Kömatex, Switzerland) were horizontally and vertically installed forming the background for the nadir and the side view camera. This procedure

Preprints (www.preprints.org) | NOT PEER-REVIEWED | Posted: 21 December 2020 doi:10.20944/preprints202012.0542.v1

allowed convenient separation of plant and background in the image. Each pot was placed in a hole of the horizontally placed plate, thereby excluding it from side view images. For the imaging from nadir view, the visible soil and pot surface was covered with blue-plate pieces, so the plant was in front of a completely blue background. Two commercially available 18 Megapixel RGB cameras (Canon EOS 600D) were installed above and beside the imaging station on a steel framework (Figure 1A) with a non-modified 22.3 x 14.9 mm sensor and a corresponding lens (Canon EF 20 mm f/2.8 USM).

For image acquisition, both cameras were simultaneously triggered with a computer-based software (DSLR remote multi-camera software, Breeze systems Ltd., UK). The cameras were set to the P-mode for imaging meaning that the camera was setting automatically shutter speed and aperture according to light conditions. The camera sensor's sensitivity to light (ISO) was set to 200 because of relatively low light intensity in the room. Automatic focus was used because of the different shapes and sizes of the plants. We used the manual focus only during very early stages of plant growth, when leaf area was insufficient to satisfy the auto focus algorithm. Metering mode was set to center-weighted average focusing on the center of the picture, where plants were located. All other settings were left as standard settings.

Imaging of plants took place at 20, 40 and 61 days after emergence and included the recording of three images, one nadir (top view) perspective and two side view perspectives with a 90° horizontal rotation to capture two different view angles on the plant shape. The traits of interest were compared to projected leaf surface measured by imaging with the nadir view, side view 1 (0°), side view 2 (90°) and with the sum of two views (nadir and side 1) and with the sum of the three views. After each imaging campaign at plant level, a subsample of imaged plants was defoliated, and the leaves were spread out (Figure 2) over a horizontal blue plate to measure total leaf surface and spectral reflectance.

2.3.2. Imaging in the field experiment

For field image acquisition a RGB camera (Canon EOS 400D) with a fixed focal length lens (Canon EF 35mm f/2 IS USM lens) was used. The camera was mounted on a self-constructed manually moveable field camera post made of aluminum pipes and connectors (Figure 1b) inspired from a device constructed by Grieder et al. [33] for field experiments. The post can be disassembled and transported easily. The camera was mounted on top of the post and images were taken from a nadir position from a height of 4 m using a remote release cable. The area of interest (AoI) used for image processing is bordered by two aluminum pipes on the left and right side at the base of the post. In the left bottom corner of this area a grey reference panel with known reflection properties (ca. 25%) (Kömatex, light grey) was attached for radiation correction of the images.

Because of bad weather conditions, imaging only started on July 5, 2018 and was continued until August 10, 2018. It was carried out on the two same representative plants per plot. Images were recorded with the manual exposure mode allowing to fix the aperture and shutter speed. The ISO was usually set to 100 and increased to 200 on cloudy days. Shutter speed and aperture were adjusted for each imaging campaign doing test images on the field and checking the average histogram for color intensities. As soon as the aperture and shutter speed fitted the light conditions, the camera was mounted on the field camera post and the position of the camera was carefully adjusted to point at the AoI.

Imaging was carried out after placing the post above the plant (nadir view for the camera) using a remote trigger taking one image per plant. Afterwards, the post was moved to the next plant and so forth. Imaging of the plants in the experimental field was carried out always in the same order to allow automated handling during post processing and analysis.

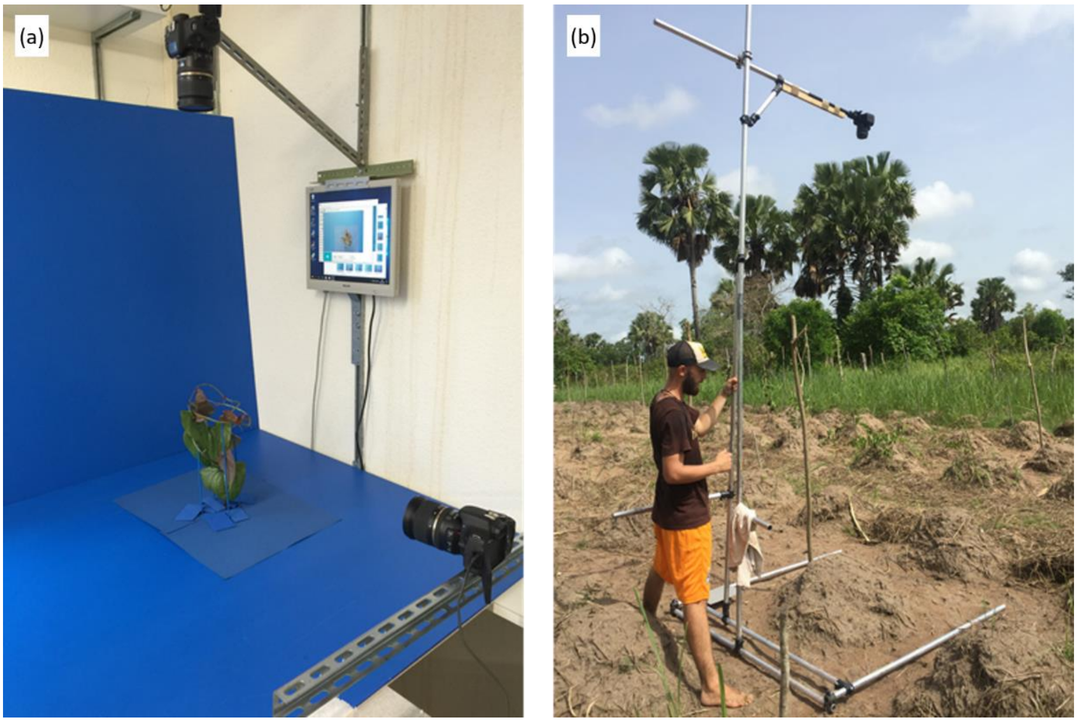

Figure 1. (**a**) Indoor imaging station with two cameras used for yam imaging at ETH Zurich plant research station in Eschikon and (**b**) the field-imaging platform with one camera in nadir view as moved over the field by the imaging operator in Côte d'Ivoire.

2.3.3. Image processing and analysis in the greenhouse and field experiment

For indoor imaging reference images without any plant were taken before each imaging series to correct for light and lens distortion. These reference images included a full blue screen image from both nadir and side view perspectives and a full screen recording of a checkerboard with known square edge length of 50 mm (Figure 2a). This procedure was repeated before each imaging campaign for plants grown in the greenhouse and the separated leaves likewise. Plant images taken from the nadir and side perspectives allowed to measure the projected leaf surface (Figure 3c), while images taken from the nadir perspective of separated leaves provided the total leaf surface (without overlapping) (Figure 2). The triangular greenness index (TGI) was calculated as shown by [12] from nadir-recorded images of separated leaves and averaged at plant level.

The rectification for lens distortion and light variation was done using a custom-made Matlab script using recorded reference images. After rectification, the images were segmented using an in-house tool. The generated output was a black and white image (mask) with plant material separated from the background and plant pixels that were counted for projected area measurements allowing for leaf surface calculation (Figures 2a, 2d, 3c). Color thresholds that separate the blue band were adjusted for each series of top- or side view images to allow best segmentation. For some series, the saturation was additionally adjusted. For this case, low saturation was also excluded during analysis because of high light intensities and reflection occurring on the blue plates.

RGB images taken in the field experiment were analyzed with the same Matlab script that was used for plants grown in the greenhouses. Therefore, images taken with the field imaging platform were cropped to the target area inside the two aluminum pipes of the field camera post base. Correction of images for light conditions was done using a grey reference plate as described above. The targeted area was segmented for vegetation using the self-learning easyPCC program developed by Guo et al. [34], allowing to count vegetation and background pixels separately. EasyPCC is a software using a decision-tree-based segmentation model (DTSM). In several images with diverse light conditions, plant material and background had to be marked manually to train the program to perform a robust segmentation on the complete data set. The generated DTSM included nine different

Preprints (www.preprints.org) | NOT PEER-REVIEWED | Posted: 21 December 2020 doi:10.20944/preprints202012.0542.v1

color features based on which single pixels were then categorized into vegetation or background [34]. The number of plant shoot pixels as well as of the soil surface cover (plant shoot pixels / total number of pixels in 1 m^2, as we have a planting density of one plant per m^2) were calculated automatically. In the field experiment, the TGI was derived from the vegetation pixels.

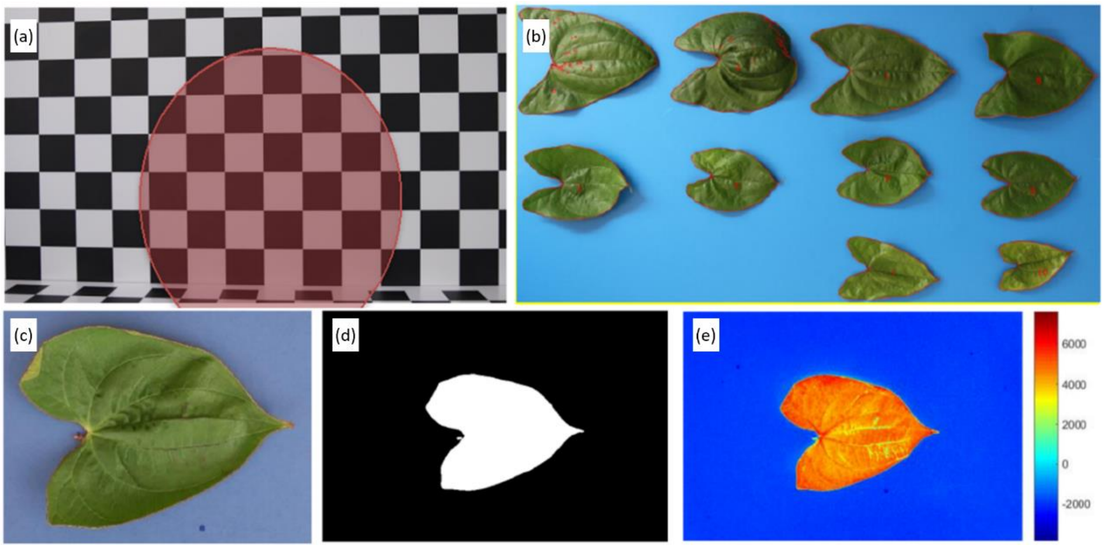

Figure 2. (**a**) Checkerboard for distortion correction, (**b**) leaves spread out on the blue plate, (**c**) single leaf, (**d**) segmented leaf, and (**e**) single leaf spectral reflectance. Red dots on leaves (**b**) indicate saturated pixels or necrotic tissue not identified as green and excluded from the spectral index analysis.

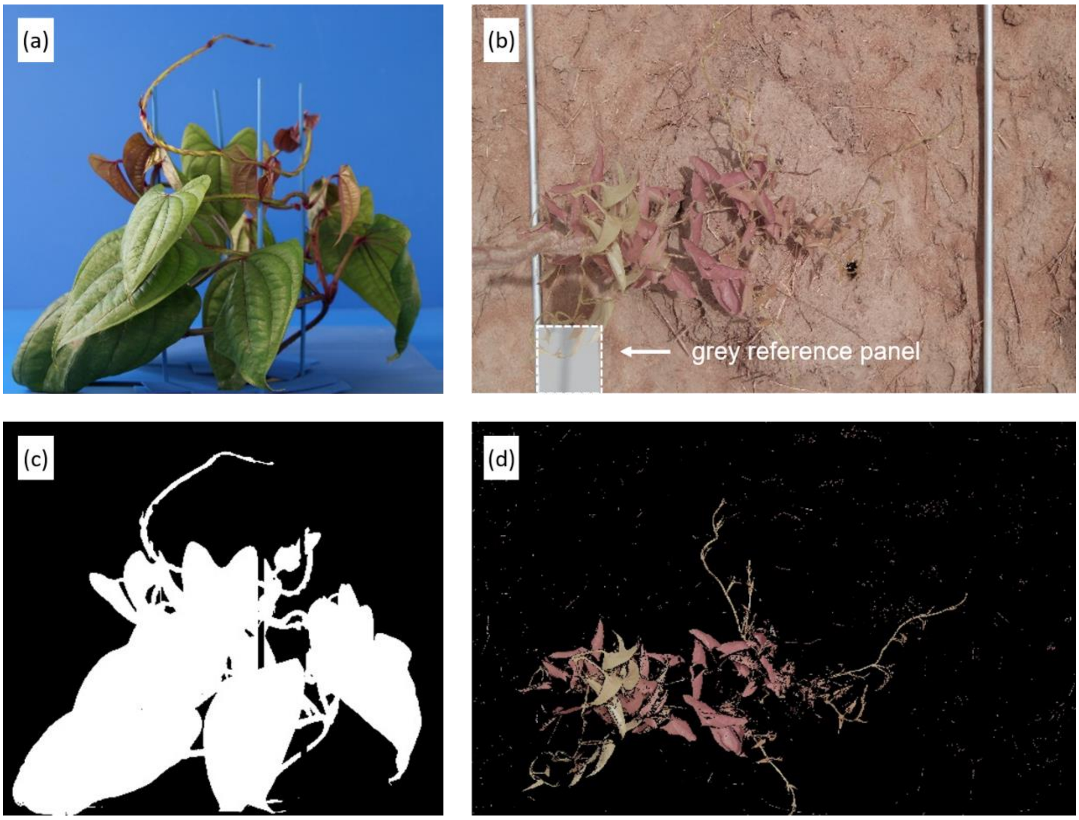

Figure 3. (**a**) Side view image of a yam plant in the indoor imaging platform, (**b**) nadir image from the field imaging platform and the corresponding segmented images (**c** and **d**), respectively.

Preprints (www.preprints.org) | NOT PEER-REVIEWED | Posted: 21 December 2020 doi:10.20944/preprints202012.0542.v1

2.4. Statistics

Statistical analysis was performed using RStudio (Version 1.0.143, 2009-2016 RStudio, Inc.). Analysis of variance (ANOVA) was performed followed by a Fisher's least significance test (LSD-posthoc test) to analyze for treatment effects in the greenhouse experiment. Data were checked for normal distribution by regarding the scale location, constant leverage, fitted values and normal Q-Q plots. All investigated data were normally distributed and thus were analyzed without transformation. The correlation between variables was assessed by calculating Pearson's correlation coefficients followed by linear regression analysis.

3. Results

3.1. Greenhouse experiment

3.1.1. Plant growth and N leaf content

We observed continuous increases in water yam aboveground fresh and dry matter, stem length, and number of leaves until 61 days after emergence (Figure 4).

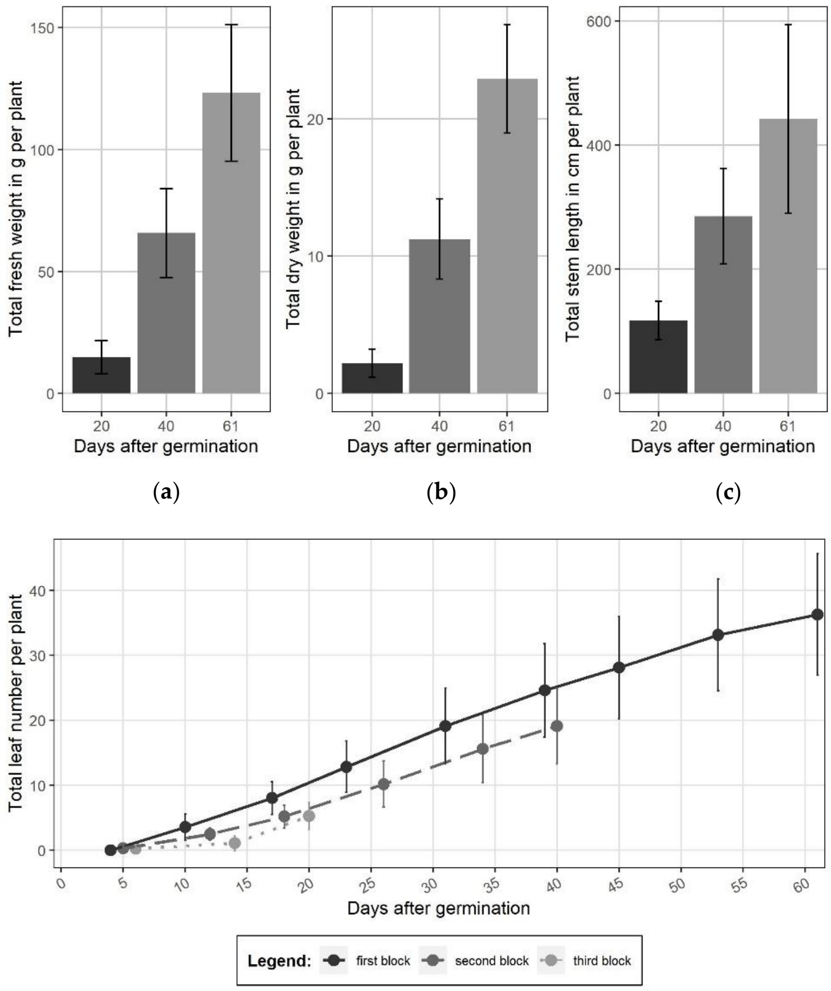

(a) (b) (c)

(d)

Figure 4. Changes with time in (**a**) total aboveground fresh weight in g per plant, (**b**) total aboveground dry weight in g per plant, (**c**) total stem length in cm per plant, and (**d**) total number of leaves per plant in water yam (cv raja ala) grown for 61 days after emergence in a greenhouse in the

Preprints (www.preprints.org) | NOT PEER-REVIEWED | Posted: 21 December 2020 doi:10.20944/preprints202012.0542.v1

presence of different N inputs. Each column represents the average measured for 20 plants, the bars show the standard deviation.

Nitrogen fertilization had no effect on the total fresh weight at 20 days after emergence but had a significant effect at 40 and, 61 days weeks after emergence (Table 1). Nitrogen concentration of the 1st and 7th fully developed leaves sampled from the apex of the main vine decreased from 20 to 61 days after emergence and N concentration was lower in the 7th leaf compared to the 1st leaf. Whereas N fertilization had little impact on the leaf N concentration at 20 days after emergence, increased N inputs led to increased N leaf content after 40 and, 61 days after emergence (Figure 5).

Table 1. Effect of N fertilization on total aboveground fresh weight (in g per plant) of water yam (cv raja ala) grown for 20, 40 and 61 days after emergence in a greenhouse. Different letters within a column indicate significant differences according to a Fisher's least significance test at *p*-level ≤ 0.05 (n = five plants per treatment).

N fertilization [kg N ha^{-1}]	**Total aboveground fresh weight g plant^{-1}**		
	20 days after emergence	40 days after emergence	61 days after emergence
0	14.16 a	48.38 b	92.66 b
50	10.02 a	66.72 ab	132.66 a
100	17.36 a	78.70 a	126.70 a
170	15.60 a	69.52 a	140.82 a

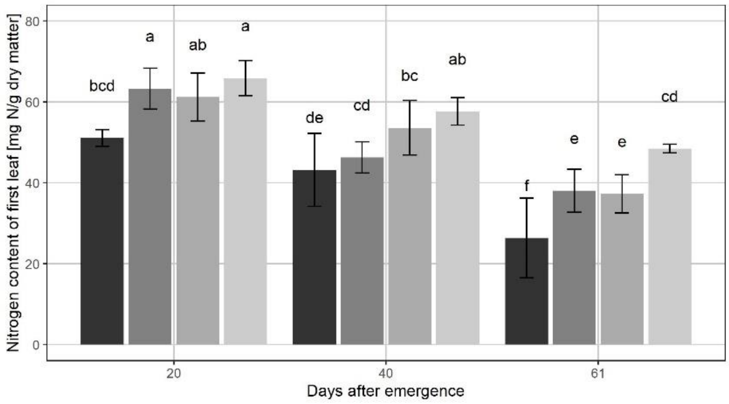

(**a**)

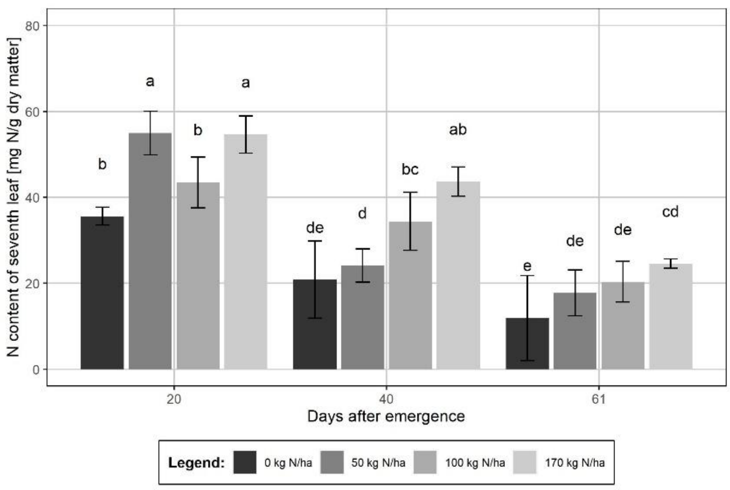

(**b**)

Preprints (www.preprints.org) | NOT PEER-REVIEWED | Posted: 21 December 2020 doi:10.20944/preprints202012.0542.v1

Figure 5. Nitrogen concentrations in the 1st (**a**) and 7th (**b**) fully developed leaves sampled from the apex of the main vine after three, six and nine weeks after germination (20, 40 and 61 days after emergence) in water yam (cv raja ala) grown in a greenhouse in the presence of different N fertilization rates. Columns show the average and the bar the standard deviation values. Letters denote significant differences calculated with least significant difference (LSD) test at *p*-level ≤ 0.05 (n = five plants per column).

3.1.2. Yam imaging

Table 2 shows that the projected leaf surface measured as the number of pixels from different points of view was highly significantly related with the traits of interest (total leaf surface, total fresh and dry weight, number of leaves and total stem length). The nadir view alone provided already excellent results. The coefficient of correlations between number of pixels (projected leaf surface) and traits of interest improved slightly with the sum of two views, while the sum of three views did not perform better than that of two views. Ringger [23] observed the same pattern in the other greenhouse experiment conducted with two water yam cultivars (see Table S1.1 in supplementary materials).

Table 2. Pearson's correlation coefficients between projected leaf area measured with the nadir view, side view 1 (0°) and 2 (90°), the sum of two views (nadir and side view 1) and the sum of three views and total leaf area, total fresh and dry weight, number of leaves and total stem length of water yam cv raja ala grown in a greenhouse during 20, 40 and 61 days after emergence in the presence of different N fertilization rates. (***) denotes significance responses on *p*-values 0.001 (n = 60 plants for each correlation).

Projected leaf surface	Total leaf surface	Total shoot fresh weight	Total shoot dry weight	Number of leaves	Total stem length
pixels plant^{-1}	cm^2 plant^{-1}	g plant^{-1}		leaves plant^{-1}	cm plant^{-1}
Nadir view	0.92***	0.95***	0.94***	0.85***	0.82***
Side 1 (0°)	0.95***	0.96***	0.96***	0.92***	0.86***
Side 2 (90°)	0.93***	0.95***	0.94***	0.90***	0.83***
Sum of 2 images	0.95***	0.97***	0.96***	0.92***	0.86***
Sum of 3 images	0.95***	0.96***	0.96***	0.92***	0.85***

The relations between the projected leaf surface measured from the nadir view and total aboveground fresh weight and total leaf area are shown in Figure 6. Whereas the variation in projected leaf surface were well explained by the variation in total shoot fresh weight or total leaf surface at 20 and 40 days after emergence, points measured after 61 days of emergence showed a higher variability. Ringger [23] observed a nonlinear regression between the projected leaf surface taken from the nadir view and the total leaf area and linear regressions between the projected leaf surface taken from the nadir view and the aboveground fresh and dry matter (Figure S1.1 in supplementary materials).

Preprints (www.preprints.org) | NOT PEER-REVIEWED | Posted: 21 December 2020 doi:10.20944/preprints202012.0542.v1

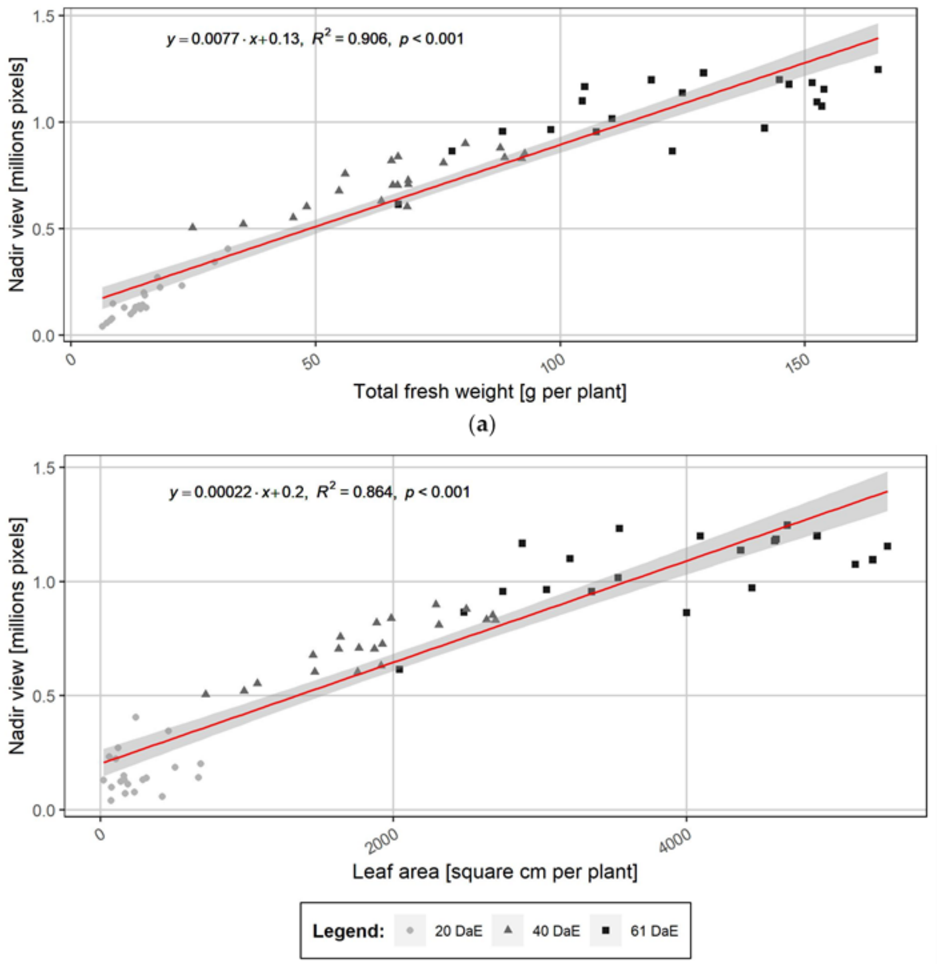

(**b**)

Figure 6. Linear regressions (**a**) between the projected leaf surface measured from the nadir view (in millions of pixels) and total shoot fresh weight (g plant^{-1}) and (**b**) between the projected leaf surface measured from the nadir view (in millions of pixels) and total leaf surface (cm^2 per plant) of water yam (cv raja ala) grown in a greenhouse in the presence of different N fertilization rates. The linear regressions, the coefficients of determination (R^2) and the *p* values are shown on each graph. The form of the symbols indicates the sampling dates: 20, 40 and 61 days after emergence (DaE) (n = 60 plants for both figures). The grey band indicates the 95% confidence interval.

The TGI values were highly significantly correlated to SPAD values (-0.67), and to the N content in the 1st and 7th fully developed leaves (Figure 7). The relations were negative as expected [12]. The points from the 20 days after emergence sampling showed for both types of leaves a higher variability around the model compared to the points obtained at 40 and 61 days after emergence. Ringger [23] also observed negative relations between TGI and N content in leaves (Figure S1.2 in supplementary materials).

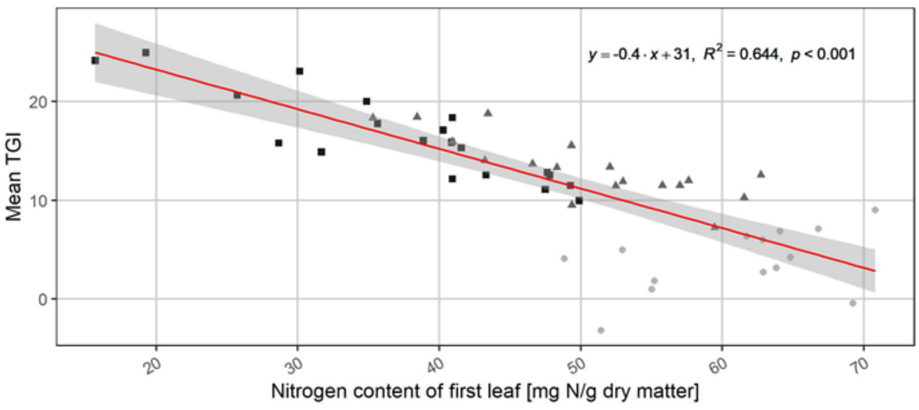

Figure 7. Relationships between the mean TGI measured at plant level and (**a**) the N content of the 1st fully developed leaf located at the apex of the main vine (n = 52 plants) and (**b**) the N content of the 7th fully developed leaf starting from the apex of the main vine (n = 58 plants) in water yam cv raja ala grown in the presence of different N fertilizations and sampled at 20, 40 and 61 days after emergence (DaE). The form of the symbols indicates the sampling dates, and the grey band indicates the 95% confidence interval.

3.2. Field experiment

3.2.1. Soil surface coverage by yam shoots

Soil surface cover (SSC) with yam shoots between July 5 and August 10 increased in average from 3.0% to 19.6% (Figure 8, Table S2.2). These changes could be modelled as highly statistically significant linear functions of time for each single plant (SSC = **a** * day + **b**) with $r^2 > 0.88$, and $p < 0.01$. As the field experiment included many treatments without replicate, we decided to present the changes in the factor **a** (% of SSC/day) in an aggregated manner, showing either the effect of fertilization using the various rotations as pseudo-replicates, or the effect of rotation using different fertilization as pseudo-replicates. The lower factor **a** observed in the non-fertilized treatment (T0) suggests that yam shoots were covering the soil less rapidly in this treatment compared to the fertilized treatments (Table 3). Similarly, the lower factor **a** observed in the rotation R3 (intercropped yam/maize – rice—yam rotation) suggests that yam shoots were covering the soil less rapidly in this treatment compared to the other rotation treatments (Table 3).

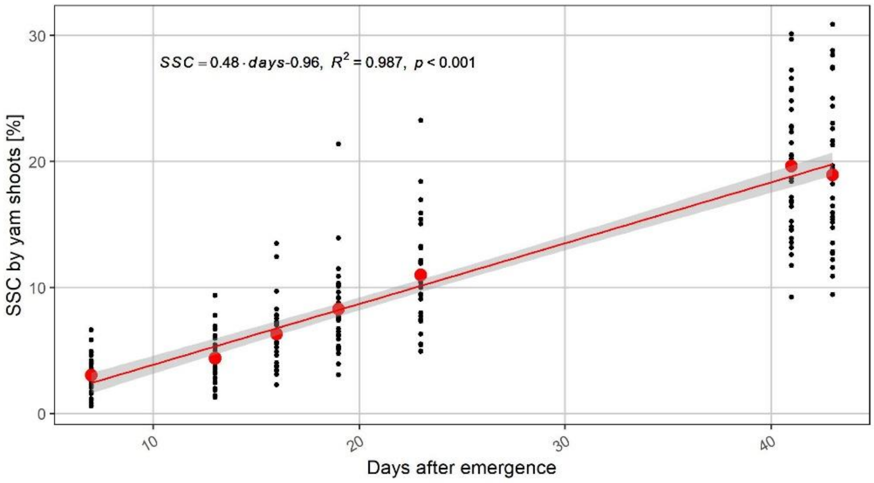

Figure 8. Relationship between the proportion of soil surface cover by yam shoots (SSC expressed in %) derived from the number of plant pixels measured in TGI images and average over all the plants and time (days after 80% of emergence) in a field experiment conducted with water yam (cv C18) in Tieningboué (Côte d'Ivoire). Each dot represents the value per plant and red dots represent the average values for all 32 plants. The grey band indicates the 95% confidence interval.

Table 3. Average and standard deviation values of the slope (**a**, expressed in SSC day^{-1}) of the linear equations describing the changes in soil surface cover by yam shoots with time between July 5 and August 10 for the various fertilization and rotation treatments implemented in a field experiment conducted with water yam (cv C18) in Tieningboué (Côte d'Ivoire). Each treatment has a n = 8 plants. Due to the absence of replicate, it was not possible to analyze these data statistically.

Preprints (www.preprints.org) | NOT PEER-REVIEWED | Posted: 21 December 2020 doi:10.20944/preprints202012.0542.v1

Treatments	a	
	average	stdev
Fertilization		
T0	0.361	0.133

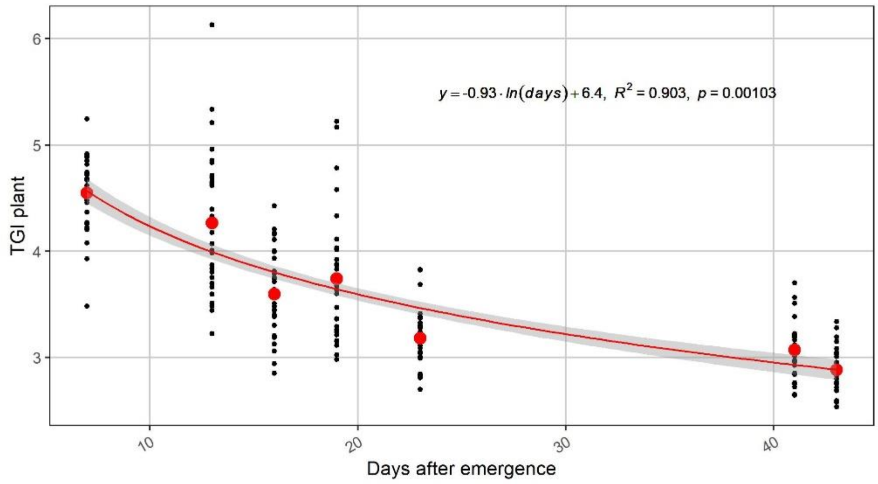

The average **a** values calculated on each of the 16 plots were weakly linearly correlated (with a *p* value of 0.0357) to the final tuber yields estimated in nearby plots submitted to the same treatments (see yields in Table S2.1 and correlation in Figure S2.2 of the supplementary materials).

3.2.2. Triangular Greenness Index

A significant nonlinear relation was observed between the average TGI values calculated for each sampling day and the number of days after germination (Figure 9).

Figure 9. Relationship between the TGI of plants measured by imaging with an RGB camera and time (days after germination) in a field experiment conducted with water yam (cv C18) in Tieningboué (Côte d'Ivoire) with different fertilizations and rotations. Each dot represents the value per plant and red dots represent the average values for all 32 plants. The grey band indicates the 95% confidence interval.

The SPAD values measured on July 14 and August 8 and 10 2018 on diagnostic leaves was negatively correlated to the TGI values measured at plant level (Figure 10), whereas no relation was observed between TGI and leaf N content, or SPAD and leaf N content measured on August 8 and 10.

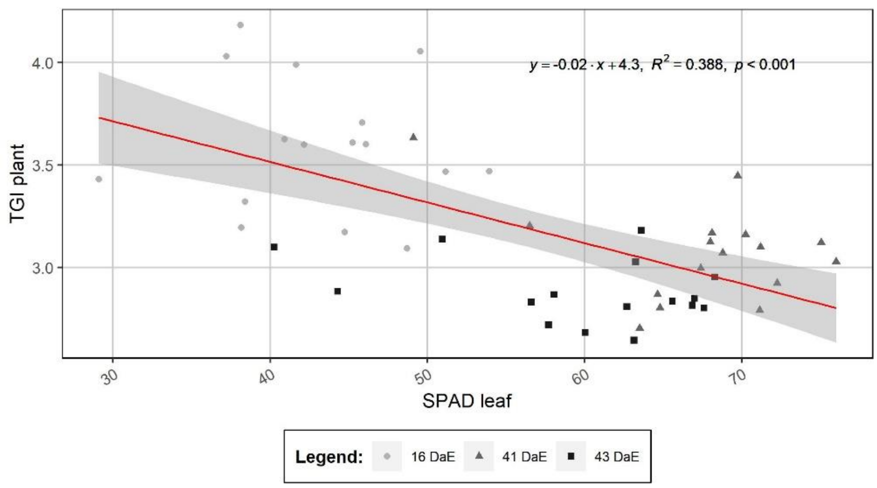

Preprints (www.preprints.org) | NOT PEER-REVIEWED | Posted: 21 December 2020 doi:10.20944/preprints202012.0542.v1

Figure 10. Relationship between the SPAD value measured on diagnostic leaves with an RGB camera and TGI of plants measured by imaging and time on July 14, August 8 and 10 (after 16, 41 and 43 days after emergence, DaE) in a field experiment conducted with water yam (cv C18) in Tieningboué (Côte d'Ivoire) with different fertilizations and rotations. Each dot represents the average values for one plot or two plants. The grey band indicates the 95% confidence interval.

4. Discussion

The results presented above show that the fixed indoor phenotyping station for greenhouse studies yielded results that robustly reflected the impact of N fertilization rates on early plant growth and N nutritional status. Furthermore, the mobile imaging of yam in the field experiment showed an increase in soil surface cover by yam shoots and a decrease of plant TGI with time. Image-based phenotyping seems therefore to generate results that are relevant for describing the early growth of yam. The discussion will touch on the limits and interests of image-based phenotyping for yam in greenhouse and field studies, and on the perspective this technique offers for yam research.

4.1. Greenhouse studies

Water yam cv raja ala grew well until 61 days after emergence in the greenhouse. Despite the large pots we used, further growth could not be studied because of the large size of the plants. Greenhouse conditions can only be used to study early yam growth, while relevant information on tuber yields can only be obtained under field conditions.

In the greenhouse, it was necessary to stack and wind the shoots around the sticks to transport them to the imaging station. This has likely limited the sensitivity of the quantification for leaf surface especially for plants with many leaves. Indeed, better coefficients of correlation were observed between the sums of pixels (i.e. the projected leaf surface) obtained from two images (nadir view plus one side view) and the measured plant traits (total leaf surface and biomass) than between the single nadir view and these plant traits (Table 2). Furthermore, the relations between these plant traits and the number of pixels obtained from the nadir view were less tight for the plants grown during 61 days after emergence than for younger plants, which was probably due to the higher number of leaves and to more leaves overlapping each other for the older plants. The nadir view alone nevertheless already reflected very well the plant traits and the differences induced by the modified N fertilization on these traits. These results also suggest that stacking and winding plants for imaging had no major negative impact on the imaging results until 61 days after emergence.

The correlation between the leaf N content and the TGI was an interesting result as the N content was measured on specific leaves while the TGI was averaged at the plant level, i.e. for the entire foliage. The same holds true for the SPAD values that were measured on diagnostic leaves and nevertheless were correlated to TGI values calculated at foliage level. This suggests that a diagnose on the N nutritional status of yam can be done by analyzing the TGI at plant level.

The fact that the two greenhouse studies yielded similar results showed that the proposed image-based phenotyping method provided repeatable results. These results suggest that imaging from the nadir view might provide relevant results both for the soil surface coverage and for assessing the N leaf content in the field.

4.2. Field study

4.2.1. Plant growth

Yam tuber yields in the field experiment conducted with the C18 cultivar were less than half of what was expected (8 to 12 t tuber ha^{-1} instead of 25 t tuber ha^{-1}). These low tuber yields were not related to an outbreak of pest, diseases or weeds as the mother tubers used for the setts and later the foliage of the growing plants were in good sanitary conditions and the field was regularly weeded. The low yields were also likely not related to an insufficient N nutrition. Indeed the N leaf content of individual plants measured in this field at 70 days after planting (41 days after emergence) ranged between 23 and 53 mg g^{-1} dry matter (mean value 35 mg g^{-1}) and had SPAD values ranging between 30 and 84 (mean value 63). Hgaza et al. [27,35] showed that fresh tuber yields of water yam cv TDa

Preprints (www.preprints.org) | NOT PEER-REVIEWED | Posted: 21 December 2020 doi:10.20944/preprints202012.0542.v1

95/00010 of 27 t ha^{-1} could be reached with leaf N content close to 33 mg g^{-1} and SPAD value of 35 measured at 75 days after planting. O'Sullivan and Jenner [26] observed a N deficiency in water yam (cv Mahoa'a) for a leaf N content lower than 20 mg g^{-1}. Note that these last works [26,27,35] measured N and SPAD values on the same leaves as in the present work. The lack of rainfall and a low soil fertility were probably also not the cause of these low water yam tuber yield as another field experiment conducted with white guinea yam cv R3 at the same site of Tieningboué delivered tuber yields higher than 20 t ha^{-1} [36]. A possible explanation for the low tuber yields observed with this water yam cultivar could be related to a low physiological quality of the C18 cultivar tuber setts used in this experiment. However, other unknown factors might have also limited yam growth during the season.

4.2.2. Imaging in the field for biomass production

Nadir imaging in the field showed that the soil surface cover by yam shoots increased linearly with time until seven weeks after emergence. This result is in agreement with the linear increase of leaf area index observed from 50 to 100 days after emergence in an improved water yam cultivar [5]. In this last work however, soil surface coverage by yam foliage reached 20 to 40% 52 days after planting [5], whereas 5 to 23% soil surface cover were observed in our field experiment at 52 days after planting (23 days after emergence). This suggests either that these two yam cultivars had different growth habits, or that plant growth was limited in our field experiment.

A weak but significant positive correlation was between the rate of soil surface cover by yam shoots during the first 43 days and the final tuber yield. This is in agreement with earlier works that found that early yam emergence and growth is positively related to tuber yield at plant level [8] but this relation needs to be validated in further field experiments.

4.2.3. Imaging in the field for estimating yam N nutritional status

The decrease of TGI during plant growth in the field suggests that N leaf content would have increased with time, as TGI and N are known to be negatively correlated with each other [12]. During the early growth phase N content in yam leaf is however supposed to decrease, as seen for example in our greenhouse experiments. Furthermore, we could not detect any relation between the TGI and the N content of leaves sampled on August 8 and 10 2018. So, the TGI decrease with time in our field experiment could not be explained by an increased N content in yam leaves. As we observed a negative correlation between TGI and SPAD, which is an estimation of leaf chlorophyll content [28], we could assign the decrease in TGI with time to an increase of chlorophyll during plant growth. The fact that leaf N content was not correlated to leaf SPAD values and to TGI values could suggest that in this field experiment N was not limiting chlorophyll production and that a variable portion of N in leaves was partitioned to other compartments than the thylakoids [37]. This absence of correlation between SPAD values and leaf N contents might also be due to variations in leaf anthocyanin content and in leaf thickness [38,39]. Yam leaves can present different anthocyanin contents, varying with the age of the leaf, the cultivar and the species, while yam leaves can also vary in thickness, e.g. by producing thinner leaves when shaded [40]. Therefore, further work must be conducted to assess the relationships between TGI, SPAD and N leaf content in yam.

4.3. Perspectives

The results obtained in this study are an important first step towards field use of imaging techniques in yam research. They show the potential of such methods to detect increase in biomass and changes in leaf composition. Yet, they need to be extended to higher replicate numbers to take the variability between plants into account. Moreover, it will be necessary to adapt the techniques described here for other important species as white yam, air yam, and lesser yam.

In the future, imaging techniques could support yam research e.g. to screen new cultivars for rapid germination and early growth as these are important drivers of final yield [7,8], and to evaluate the impact of cropping systems (rotation, fertilization…) on canopy development. Altogether, this information will support the development of models predicting tuber yield based on pedo-climatic variables, cultivar, and management.

These imaging techniques will be useful to adapt yam cropping systems to local conditions. Indeed, given the high diversity of yam cropping systems [1] there is no one suits all solution [4,6]. Appropriate site-specific innovations need to be designed, tested, and validated with local stakeholders [6]. If this is done, there is a chance that farmers will adopt innovations and sustainably improve yam productivity in their fields [4].

Supplementary Materials: The following are available online at www.mdpi.com/xxx/s1,

Table S1.1: Pearson's correlation coefficient of projected leaf area assessed from the nadir (top) view, side view 0°, side view 90°, the sum of two views (nadir and side 0°) and the sum of three views and destructively measured total leaf area, dry weight and fresh weight measured on two genotypes of water yam (raja ala and florido, n=24 genotype^{-1}) grown in the greenhouse under three nitrogen fertilizer treatments (0, 50 and 170 kg N ha^{-1}) and harvested six and eight weeks after emergence. Leaf area was transformed prior to the calculation using the natural logarithm; **Figure S1.1:** Relation between projected leaf surface calculated from single top (nadir) images, and destructively measured total leaf surface a), shoot dry weight b), and shoot fresh weight c) for two genotypes of water yam (SL, CI, n=24 genotype^{-1}) grown in the greenhouse under three nitrogen fertilizer treatments (0, 50 and 170 kg N ha^{-1}) and harvested six and eight weeks after emergence; **Figure S1.2:** Relation between SPAD value and leaf nitrogen (N) content at different leaf positions (leaf no. 1, 8, 16, counted from base to apex) A) and between TGI value (triangular greenness index) and leaf nitrogen (N) content at different leaf positions (leaf no. 1, 8, 16, counted from base to apex) B) in water yam cv raja ala, six and eight weeks after emergence (wae). Plants were grown under three nitrogen treatments (0, 50, 170 kg N ha^{-1}) in a greenhouse. Regression lines were included, when results were significant (p-value <= 0.05); **Figure S2.1:** Climate diagram of the season 2018 for Tieningboué. The mean temperature (°C) is shown by the red line, the maximum temperature by the upper black line and the minimum temperature by the lower black line. The precipitation (mm) is shown with bar plots. No weather data was available for 22 days in March and 22 days in April 2018; **Table S2.1**: Tuber yield (average and standard error) of water yam cv C18 measured in a nearby experiment located on the same soil and submitted to the same treatments (rotation R1 to R4 and fertilization T0 to T3, see details in the paper) as those studied in our field experiment; **Table S2.2**: Soil surface coverage (%) measured from pixel numbers obtained from TGI image for each studied plant between July 5 2018 and August 10, 2018 in our field experiment; **Figure S2.2:** Relationship between final tuber yields and the average daily rate of soil surface coverage by yam shoots (**a**) between July 5 and August 10, 2018 in our field experiment; **Table S2.3**: TGI measured at plant level for each studied plant between July 5 2018 and August 10, 2018 in our field experiment.

Author Contributions: Conceptualization, E.F and F.L.; imaging methodology, F.L., N.K., A.W; software, N.K., A.W.; greenhouse house experiments, C.R., L.M.; field experiment, L.M., N.P., V.H., D.K.; writing—original draft preparation, E.F., F.L.; writing—review and editing, all authors; visualization, L.M., C.R..; supervision, E.F., F.L., V.H., D.K.; project administration, E.F.; funding acquisition, E.F. All authors have read and agreed to the published version of the manuscript.

Funding: This research was funded in the frame of the food security module of the "Swiss program for research on global issues for development" by the SNF and the SDC (YAMSYS project, SNF project number: 400540_152017 / 1).

Acknowledgments: The authors warmly thank Monika Macsai, and Laurie Schönholzer from the group of plant nutrition of the ETH and Brigitta Herzog from the group of crop science of ETH for their support in the greenhouse experiments as well as the members of the YAMSYS field crew in Tieningboué for their help.

Conflicts of Interest: The authors declare no conflict of interest. The funder had no role in the design of the study; in the collection, analyses, or interpretation of data; in the writing of the manuscript, or in the decision to publish the results.

References

1. Lebot, V. *Tropical Root and Tuber Crops; Cassava, Sweet Potato, Yams and Aroids*, 2nd Edition, CIRAD, CABI, Wallingford, Oxfordshire, UK, 2020.

2. Sangakkara, U.R.; Frossard, E. Home gardens and Dioscorea species – A case study from the climatic zones of Sri Lanka. *Journal of Agriculture and Rural Development in the Tropics and Subtropics (JARTS)* **2014**, 115, 55–65.
3. Nweke, F.I. *Yam in West Africa, food money and more*, Michigan State University Press, East Lansing, USA, 2016.
4. Frossard, E.; Aighewi, B.; Aké, S.; Barjolle, D.; Baumann, P.; Bernet, T.; Dao, D.; Diby, L.N.; Floquet, A.; Hgaza, V.K.; Ilboudo, L.J.; Kiba, D.I.; Mongbo, R.L.; Nacro, H.B.; Nicolay, G.; Oka, E.; Ouattara, Y.F.; Pouya, N.; Senanayake, R.L.; Six, J.; Traoré, O.I. The challenge of improving soil fertility in yam cropping systems of West Africa. *Front Plant Sci - Agroecology and Land Use Systems* **2017**, 8, 1953, doi: 10.3389/fpls.2017.01953.
5. Diby, L.N.; Hgaza, V.K.; Tié, T.B.; Assa, A.; Carsky, R.; Girardin, O.; Sangakkara, U.R.; Frossard, E. How does soil fertility affect yam growth? *Acta Agric Scand B Soil Plant Sci* **2011**, 61, 448-457.
6. Kiba, D.I.; Hgaza, V.K.; Aighewi, B.; Aké, S.; Barjolle, D.; Bernet, T.; Diby, L.N.; Ilboudo, L.J.; Nicolay, G.; Oka, E.; Ouattara, F.Y.; Pouya, N.; Six, J.; Frossard, E. A transdisciplinary approach for the development of sustainable yam (*Dioscorea* sp.) production in West Africa. *Sustainability* **2020**, 12, 4016; doi:10.3390/su12104016.
7. Cornet, D.; Sierra, J.; Tournebize, R.; Ney, B. Yams (*Dioscorea* spp.) plant size hierarchy and yield variability: Emergence time is critical. *Eur J Agron* **2014**, 55, 100–107.
8. Cornet, D.; Sierra, J.; Tournebize, R.; Gabrielle, B.; Lewis, F.I. Bayesian network modeling of early growth stages explains yam interplant yield variability and allows for agronomic improvements in West Africa. *Eur J Agron* **2016**, 75, 80–88, doi: 10.1016/j.eja.2016.01.009.
9. Hgaza, V.K., Oberson, A., Kiba, D.I., Diby, L.N., Aké, S., Frossard E. The nitrogen nutrition of yam (*Dioscorea* spp). *J Plant Nutr* **2020**, 43, 64-78, doi.org/10.1080/01904167.2019.1659315.
10. Buerkert, A.; Lawrence, P.R.; Williams, J.H.; Marschner, H. Nondestructive measurements of biomass in millet, cowpea, groundnut, weeds and grass swards using reflectance, and their application for growth analysis. *Exp Agric* **1995**, 31, 1-11.
11. Buerkert, A.; Mahler, F.; Marschner, H. Soil productivity management and plant growth in the Sahel: Potential of an aerial monitoring technique. *Plant Soil* **1996**, 180, 29-38.
12. Hunt, E.R.; Daughtry, C.S.T.; Eitel, J.U.H.; Long, D.S. Remote sensing leaf chlorophyll content using a visible band index. *Agron J* **2011**, 103, 1090–1099 doi: 10.2134/agronj2010.0395.
13. Kirchgessner, N.; Liebisch, F.; Yu, K.; Pfeifer, J.; Friedli, M.; Hund, A.; Walter, A. The ETH field phenotyping platform FIP: a cable-suspended multi-sensor system. *Funct Plant Biol* **2017**, 44, 154-168.
14. Joalland, S.; Screpanti, C.; Gaume, A.; Walter, A. Belowground biomass accumulation assessed by digital image based leaf area detection. Plant Soil **2016,** 398; 257-266.
15. Joalland, S.; Screpanti, C.; Liebisch, F.; Varella, H.V.; Gaume, A.; Walter, A. Comparison of visible imaging, thermography and spectrometry methods to evaluate the effect of *Heterodera schachtii* inoculation on sugar beets. *Plant Methods* **2017**, 13, 73 DOI: 10.1186/s13007-017-0223-1.
16. Li, B.; Xu, X.; Han, J.; Zhang L.; Bian C.; Jin L.; Liu J. The estimation of crop emergence in potatoes by UAV RGB imagery. *Plant Methods* **2019**, 15, 15 https://doi.org/10.1186/s13007-019-0399-7.
17. Hunt, E.R.; Horneck, D.A.; Spinelli, C.B.; Turner, R.W.; Bruce, A.E.; Gadler, D.J.; Brungardt, J.J.; Hamm, P.B. Monitoring nitrogen status of potatoes using small unmanned aerial vehicles. *Precis Agric* **2018**, 19, 314-333.
18. Liebisch, F; Kirchgessner, N; Schneider, D; Walter, A; Hund, A. Remote, aerial phenotyping of maize traits with a mobile multi-sensor approach. *Plant Methods* **2015**, 11, 9, DOI: 10.1186/s13007-015-0048-8.
19. Iseki, K.; Matsumoto, R. Non-destructive shoot biomass evaluation using a handheld NDVI sensor for field-grown staking Yam (*Dioscorea rotundata* Poir.). *Plant Prod Sci* **2019**, 22, 301-310, DOI: 10.1080/1343943X.2018.15402782.
20. Kolade, O.A.; Oguntade, O.; Kumar, L. Screening for resistance to Yam Anthracnose Disease. Virology/Germplasm Health Unit, IITA Ibadan, **2018** https://africayam.org/download/screening-resistance-yam-anthracnose-disease/ (accessed on sept 24 2020).
21. Ramcharan, A.; Baranowski, K.; McCloskey, P.; Ahmed, B.; Legg, J.; Hughes, D.P. Deep Learning for Image-Based Cassava Disease Detection. *Front Plant Sci* **2017**, 8, 1852.

22. Darkwa, K.; Olasanmi, B.; Asiedu, R.; Asfaw, A. 2019 Review of empirical and emerging breeding methods and tools for yam (*Dioscorea* spp.) improvement: Status and prospects. *Plant Breed*, **2020**, 139, 474-497, DOI: 10.1111/pbr.12783.
23. Ringger, C. Development of a digital method to assess shoot development of yam (*Dioscorea* spp.) at early vegetative stage. Master of Science Thesis, ETH Zürich, 2018.
24. Müller, L. Digital Phenotyping of yam (*Dioscorea* sp.) under glasshouse and field conditions. Master of Science Thesis, ETH Zürich, 2017.
25. Aighewi, B.A.; Maroya, N.G.; Asiedu, R. Seed yam production from minisetts : A training manual. International Institute for Tropical Agriculture, Ibadan, Nigeria, 2014.
26. O'Sullivan, J.N.; Jenner, R. Nutrient deficiencies in greater yam and their effects on leaf nutrient concentrations. *J Plant Nutr* **2006,** 29, 1663–1674. doi: 10.1080/01904160600851569
27. Hgaza, V.K.; Diby, L.N.; Aké, S.; Frossard E. Leaf growth and photosynthetic capacity as affected by leaf position, plant nutritional status and growth stage in *Dioscorea alata* L. *J Anim Plant Sci* **2009**, 5, 483 - 493.
28. Hawkins, T.S.; Gardiner, E.S.; Comer, G.S. Modeling the relationship between extractable chlorophyll and SPAD-502 readings for endangered plant species research. *J Nat Conserv* **2009**, 17, 125-129.
29. Müller, P. Measurement of leaf surface area, soil cover and N content in leaves of field-grown yams (*Dioscorea* spp). Master of Science Thesis, ETH Zürich, 2018.
30. WRB. *International soil classification system for naming soils and creating legends for soil maps*. World Soil Resource Reports, FAO, Roma, Italy 2014.
31. Schneider, K. *Soil characterization of YAMSYS sites*. Internal YAMSYS report, 2018 (available on request).
32. Doumbia, S.; Koko, L.; Aman, S.A. L'introduction et la diffusion de la variété d'igname C18 en région centre de Côte d'Ivoire. *J Appl Biosci* **2014,** 80, 7121–7130 doi: 10.4314/jab.v80i1.2.
33. Grieder, C.; Hund, A.; Walter, A. Image based phenotyping during winter: a powerful tool to assess wheat genetic variation in growth response to temperature. *Funct Plant Biol* **2015,** 42, 387–396 Doi 10.1071/Fp14226.
34. Thenkabail, P.S.; Lyon, J.G. *Hyperspectral Remote Sensing of Vegetation*, 1st ed.; CRC Press, Boca Raton, US, 2012 DOI https://doi.org/10.1201/b11222.
35. Sims, D.A.; Gamon, J.A. Relationships between leaf pigment content and spectral reflectance across a wide range of species, leaf structures and developmental stages. *Remote Sens Environ* **2002**, 81, 337-354.
36. Guo, W.; Zheng, B.; Duan, T.; Fukatsu, T.; Chapman, S.; Ninomiya, S. EasyPCC: Benchmark Datasets and Tools for High-Throughput Measurement of the Plant Canopy Coverage Ratio under Field Conditions. *Sensors* **2017**, 17, 798.
37. Hgaza, V.K.; Diby, L.N.; Oberson, A.; Tschannen, A.; Tié, B.T.; Sangakkara, U.R.; Aké, S.; Frossard, E. Nitrogen Use by Yam as Affected by Mineral Fertilizer Application. *Agron J* **2012**, 104, 1558-1568.
38. Hgaza, H.K. (Département d'Agrophysiologie des Plantes, Université Peleforo Gon Coulibaly, Korhogo, Côte d'Ivoire) personal communication 2018.
39. Diby, L.N.; Tie, B.T.; Girardin, O.; Sangakkara, U.R.; Frossard, E. Growth and nutrient use efficiencies of yams (*Dioscorea* spp.) grown in two contrasting soils of West Africa. *Int J Agron* **2011**, article ID 175958, doi:10.1155/2011/175958.
40. Evans, J.R. Photosynthesis and nitrogen relationships in leaves of C3 plants. Oecologia **1989**, 78, 9-19.
41. Manetas, Y.; Grammatikopoulos, G.; Kyparissis, A. The use of the portable, non-destructive, SPAD-502 (Minolta) chlorophyll meter with leaves of varying trichome density and anthocyanin content. *J Plant Physiol* **1998**, 153, 513-516.
42. Jifon, J.L.; Syvertsen, J.P.; Whaley, E. Growth environment and leaf anatomy affect nondestructive estimates of chlorophyll and nitrogen in *Citrus* sp leaves. *J Am Soc Hortic Sci* **2005**, 130, 2, 152-158.
43. Onwueme, I.C.; Johnston, M. 2000 Influence of shade on stomatal density, leaf size and other leaf characteristics in the major tropical root crops, tannia, sweet potato, yam, cassava and taro. *Exp Agric* **2000**, 36, 509-516.